

Microwave dielectric properties of graded barium strontium titanate films

M. W. Cole,^{1,a)} C. V. Weiss,² E. Ngo,¹ S. Hirsch,¹ L. A. Coryell,³ and S. P. Alpay^{2,b)}

¹Weapons and Materials Research Directorate, Active Materials Research Group, U.S. Army Research Laboratory, Aberdeen Proving Ground, Maryland 21005, USA

²Materials Science and Engineering Program and Institute of Materials Science, University of Connecticut, Storrs, Connecticut 06269, USA

³Space and Terrestrial Communications Directorate, U.S. Army Communications and Electronics Research Development and Engineering Center, Fort Monmouth, New Jersey 07703, USA

(Received 8 April 2008; accepted 13 April 2008; published online 8 May 2008)

Compositionally graded barium strontium titanate ($\text{Ba}_x\text{Sr}_{1-x}\text{TiO}_3$ or BST) multilayers (5 mol % MgO doped and undoped) were prepared via metallo-organic solution deposition on Pt–Si substrates and characterized electrically at 0.5, 5, and 10 GHz. For the undoped BST multilayers, the small-signal dielectric response, tunability, and the loss tangent at 10 GHz were 261, 25% at 1778 kV/cm, and 0.078, respectively. On the other hand, the Mg-doped BST multilayers displayed a significant improvement in the loss characteristics at 10 GHz (0.039) but the dielectric response and its tunability were lower (189 and 15%, respectively, at 1778 kV/cm). © 2008 American Institute of Physics. [DOI: 10.1063/1.2919080]

Ferroelectric materials have been the subject of intense research for use in a variety of applications due to their unique ferroelectric, piezoelectric, and pyroelectric properties. A potential application of ferroelectric materials is in microwave tunable devices, including tunable mixers, delay lines, filters, and phase shifters for steerable antennas.^{1–3} Barium strontium titanate ($\text{Ba}_x\text{Sr}_{1-x}\text{TiO}_3$ or BST) has become the leading materials system for these devices due to its high dielectric response and its tunability near the ferroelectric phase transformation temperature T_C (see Ref. 4 for an excellent review). The transition temperature can be controlled via adjusting composition. For example, the T_C of bulk BST 60/40 ($\text{Ba}_{0.60}\text{Sr}_{0.40}\text{TiO}_3$) is just below room temperature (5 °C). By adjusting the composition of BST films, the transition temperature and, hence, the dielectric properties and its tunability can be tailored. Therefore, several compositions of BST thin films have been studied in great detail for use in tunable microwave devices using a variety of different fabrication methods and substrates.^{5–11}

To be utilized in such devices, thin films of BST must have a high tunability, a low loss tangent in the microwave regime, and a dense crack-free microstructure, accompanied by a minimal dispersion in dielectric properties over a large temperature interval (–20–+85 °C).² Introducing a composition gradient has been identified as one way of reducing the temperature dependence of the dielectric response and its tunability.¹² Theoretically, multilayer BST films with systematic variations in the composition and graded ferroelectrics should display little temperature dependence in the dielectric behavior due to the variations in T_C that result in a “diffuse” phase transformation. The tunability can then be maximized by optimizing the internal electric fields that arise between layers due to the polarization mismatch.¹³ Furthermore, it has been shown that losses in BST can be reduced via acceptor doping.¹⁴ Dopants (such as Ni^{2+} , Al^{2+} , Ga^{3+} , $\text{Mn}^{2+,3+}$, $\text{Fe}^{2+,3+}$, Mg^{2+} , etc.) typically occupy the *B* site of the ABO_3

perovskite structure, substituting for Ti^{4+} ions. The charge difference between the dopant and Ti^{4+} can effectively compensate for oxygen vacancies and thereby have been shown to decrease dielectric losses.¹⁵

Therefore, a combination of both methods presents an opportunity to develop materials for tunable device applications with temperature insensitive dielectric properties and low losses. Indeed, our recent experimental results show that BST multilayer heterostructures consisting of three distinct layers of ~220 nm nominal thickness with compositions corresponding to $\text{Ba}_{0.6}\text{Sr}_{0.4}\text{TiO}_3$ (BST 60/40), BST 75/25, and BST 90/10 on Pt-coated Si substrates have a small-signal dielectric permittivity of 360 with a dissipation factor of 0.012 and a dielectric tunability of 65% at 444 kV/cm when tested at 100 kHz. These properties exhibit minimal variation as a function of temperature ranging from 90 to –10 °C. Furthermore, it was shown that Mg doping improves dielectric loss ($\tan \delta=0.008$) compared to undoped graded BST, although, this also results in a moderate dielectric tunability (29%) compared to undoped multilayer BST (65.5%) at 444 kV/cm.¹⁶ Similar to undoped BST multilayers, Mg-doped BST multilayers display excellent temperature stability with temperature coefficient of capacitances (TCCs) of –0.94 and 1.14 ppt/°C from 20 to 90 °C and –10 to 20 °C, respectively.^{16,17} Since tunable devices for telecommunications are operated in the microwave range (300 MHz to 300 GHz), it is important to test the dielectric properties of these materials at higher frequencies. In this letter, we report dielectric properties of Mg-doped and undoped multilayer BST heterostructures at gigahertz frequencies and show that a high dielectric tunability (15%–25% at 1778 kV/cm) and low losses (0.04–0.08) can be maintained even at such high frequencies.

Multilayer doped and undoped BST thin films of approximately 225 nm nominal thickness were prepared by metallo-organic solution deposition (MOSD) on Pt-coated Si substrates. Barium acetate, strontium acetate, magnesium acetate, and titanium (IV) isopropoxide were used to create the carboxylate-alkoxide precursor solution for BST with the proper stoichiometry. A detailed description of precursor so-

^{a)}Electronic mail: mcole@arl.army.mil.

^{b)}Author to whom correspondence should be addressed. Electronic mail: p.alpay@ims.uconn.edu.

lution preparation and the synthesis have been reported elsewhere.¹⁵ The compositionally graded BST thin film consisted of three compositionally distinct layers of $\sim 72\text{--}74$ nm thickness corresponding to BST60/40, BST75/25, and BST90/10. These films are upgraded (UG), which means that BST60/40 is deposited on the substrate first, followed by the BST75/25 and BST90/10 layers. After the spin-on film coating, the sample was pyrolyzed at 350°C for 10 min to remove the organic addenda. After each individual spin-on film coating, the sample was annealed at 750°C for 1 h to ensure that the layer was crystallized prior to the deposition of the next compositionally distinct layer.

A detailed crystallographic and microstructural characterization has been carried out via x-ray diffraction (XRD), atomic force microscopy (AFM), field-emission scanning electron microscopy, and Raman backscattering, and these findings were reported in detail elsewhere.¹⁵ Here, we shall provide a short summary regarding the surface morphology and microstructure of these films. XRD data revealed that the samples had a random polycrystalline perovskite structure and there were no secondary phases present. AFM results showed that the films had a dense microstructure with no cracks, pinholes, or other surface defects. The Mg doping resulted in a decrease in the grain size (72 nm for undoped graded BST and 60 nm for Mg-doped graded BST), which in turn affected the surface roughness. Mg-doped UG-BST films had a surface roughness of ~ 3.1 nm compared to ~ 3.5 nm for undoped UG-BST films.¹⁶ We note that a low surface roughness promotes better contact properties, reduces insertion losses, and is thus a desirable characteristic in tunable devices.

Electrical measurements were carried out at frequencies ranging from 0.5 to 10 GHz using a coplanar interdigitated capacitor (IDC) device configuration with $4\text{--}8\ \mu\text{m}$ finger gaps and $80\ \mu\text{m}$ finger lengths. The IDCs, composed of Ag ($1.5\ \mu\text{m}$ thick) with a thin adhesion layer of Cr and a protective capping layer of Au, were deposited onto the films using a polymethyl methacrylate lift-off mask and electron beam evaporation. The microwave dielectric properties of the BST films were measured as a function of frequency (0.5–10 GHz) and dc bias ($-40\text{--}40$ V) by using a $200\ \mu\text{m}$ pitch Picoprobe microwave probe with an HP 8510C network analyzer. Reflection curve measurements (S_{11}) were fitted to a parallel resistor-capacitance model to obtain capacitance (C) and device quality factor (Q). The relative dielectric response (ϵ_r) and dielectric loss ($\tan \delta$) were calculated from the capacitance, device Q , and IDC dimensions with a conformal mapping technique.¹⁸

In Fig. 1, we plot the relative dielectric permittivity as a function of the applied bias at 0.5, 5, and 10 GHz for the undoped UG-BST and the Mg-doped UG-BST. The permittivity decreases with an increase in the testing frequency. The permittivity is significantly lower at all frequencies for the Mg-doped UG BST film. For example, at 10 GHz, the dielectric response of UG-BST is 261, whereas it is 189 in Mg-doped BST. This is expected as Mg additions are known to lower the ferroelectric transformation temperature, as shown by Su and Button in bulk ceramic BST.¹⁹ The relative displacement of Ti^{4+} cations results in a permanent dipole and thus ferroelectric behavior in BST. Mg^{2+} cations substitute for Ti^{4+} in the prototypical perovskite BST lattice. This, combined with the volumetric expansion with the addition of MgO to BST,¹⁶ can be possible reasons for the suppression

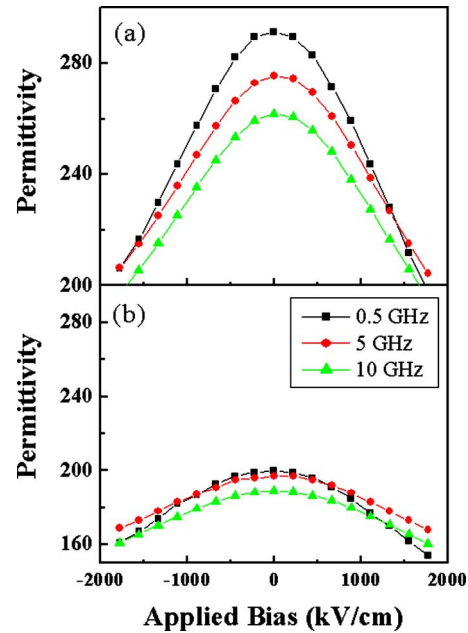


FIG. 1. (Color online) Relative dielectric permittivity as a function of the applied bias at 0.5, 5, and 10 GHz for (a) undoped UG-BST and (b) Mg-doped UG-BST.

of ferroelectricity. Furthermore, a smaller grain size might also lower the dielectric response.²⁰

The dielectric losses were also measured at microwave frequencies. In Fig. 2, we plot the microwave dielectric loss as a function of applied electric field at 0.5, 5, and 10 GHz for the UG and the Mg-doped UG BST films. As expected, we find that as the frequency increases, the loss increases. We note that the loss is lower at each frequency in the Mg-doped film. For example, the loss at 10 GHz in the undoped film is 0.078 compared to 0.039 in the Mg-doped heterostructure at the same frequency. While both values are significantly larger than the loss at 100 kHz (0.008),¹⁶ these still are within acceptable tolerances for tunable devices. The increase in the dielectric losses in the microwave frequency

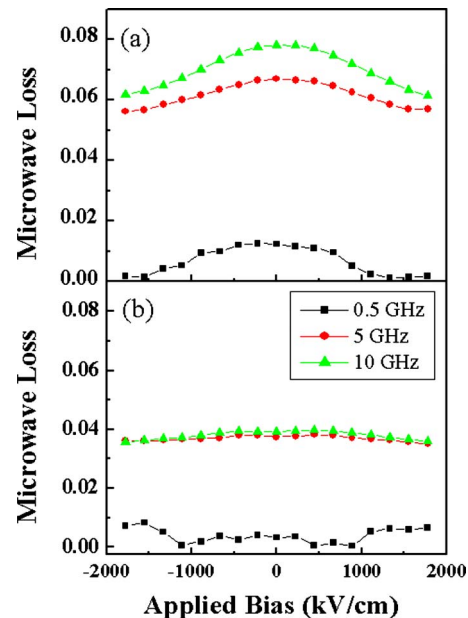


FIG. 2. (Color online) Microwave loss as a function of the applied bias at 0.5, 5, and 10 GHz for (a) undoped UG-BST and (b) Mg-doped UG-BST.

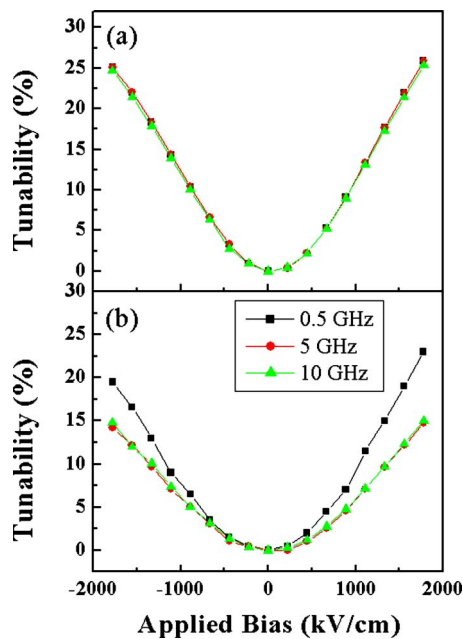


FIG. 3. (Color online) High frequency tunability as a function of applied bias at 0.5, 5, and 10 GHz for (a) undoped UG-BST and (b) Mg-doped UG-BST.

range can be thought of to be due to a number of reasons, both of intrinsic (due to the interaction of the ac field phonons, including quasi-Debye losses) and of extrinsic (e.g., mobile charged defects, such as oxygen vacancies) nature.²

Figure 3 shows the dielectric tunability as a function of the applied electric field at 0.5, 5, and 10 GHz for both the undoped UG-BST and the Mg-doped UG-BST. In the undoped UG-BST, the tunability displays little frequency dependence and is $\sim 25\%$ at 1778 kV/cm for all the test frequencies. In the Mg-doped films, the tunability at 1778 kV/cm decreases from 23% at 0.5 GHz to 15% at 10 GHz. This was also observed at 100 kHz in identical samples; 65% vs 29% at 444 kV/cm for graded and Mg-doped graded films, respectively.¹⁶ This reduction in the tunability is related to the decrease in the dielectric response with Mg doping, as discussed above.

There is a substantial decline in the tunability of both samples at gigahertz frequencies compared to the previous report where the electrical measurements were carried out at 100 kHz.¹⁶ This behavior may not be entirely intrinsic. It is well known that one can expect a precipitous fall in the dielectric response (and hence its tunability) at higher frequencies for materials where the significant portion of the polarization is due to ionic displacements and/or molecular rearrangement in the presence of an external field. However, the decrease in the tunability in the current study and the one

previously reported at 100 kHz can also be related to completely different device geometries (IDC versus parallel plate). Since the device geometry is coplanar, the tunability that is reported here for gigahertz frequencies is actually the lower limit since only a portion (typically less than 50%) of the field is confined within the film.²¹ In other words, parallel plate varactor structures offer higher tunability compared to the coplanar IDC structures since the electric fields are fully confined within the film, as compared to IDCs. These suffer from reduced tunability due to the large fringing field in the air, hence may not be confined within the active material of the device structure. Thus, the tunability is considerably lower than if this were in a parallel plate configuration. The results would be significantly improved if the total applied field were confined and thus fully utilized to tune the material in a parallel plate varactor configuration.

The work at UConn was supported by the U.S. Army Research Office through Grant No. W911NF-05-1-0528.

- ¹M. J. Lancaster, J. Powell, and A. Porch, *Supercond. Sci. Technol.* **11**, 1323 (1998).
- ²A. K. Tagantsev, V. O. Sherman, K. F. Astafiev, J. Venkatesh, and N. Setter, *J. Electroceram.* **11**, 5 (2004).
- ³O. G. Vendik, E. K. Hollmann, A. B. Kozyrev, and A. M. Prudan, *J. Supercond.* **12**, 325 (1999).
- ⁴P. Bao, T. J. Jackson, X. Wang, and M. J. Lancaster, *J. Phys. D* **41**, 063001 (2008).
- ⁵X. H. Zhu, N. Chong, H. L. W. Chan, C. L. Choy, K. H. Wong, Z. Liu, and N. Ming, *Appl. Phys. Lett.* **80**, 3376 (2002).
- ⁶S. G. Lu, X. H. Zhu, C. L. Mak, K. H. Wong, H. L. W. Chan, and C. L. Choy, *Appl. Phys. Lett.* **82**, 2877 (2003).
- ⁷A. Lookman, R. M. Bowman, J. M. Gregg, J. Kut, S. Rios, M. Dawber, A. Ruediger, and J. F. Scott, *J. Appl. Phys.* **96**, 555 (2004).
- ⁸J. Bellotti, E. K. Akdogan, A. Safari, W. Chang, and S. Kirchoefer, *Integr. Ferroelectr.* **49**, 113 (2002).
- ⁹M. Jain, S. B. Majumder, R. S. Katiyar, A. S. Bhalla, F. A. Miranda, and F. W. Van Keuls, *Appl. Phys. A: Mater. Sci. Process.* **80**, 645 (2005).
- ¹⁰J. Sigman, P. G. Clem, C. D. Nordquist, J. J. Richardson, and J. T. Dawley, *J. Appl. Phys.* **102**, 054106 (2007).
- ¹¹E. A. Fardin, A. S. Holland, K. Ghorbani, E. K. Akdogan, W. K. Simon, A. Safari, and J. Y. Wang, *Appl. Phys. Lett.* **89**, 182907 (2006).
- ¹²Z. G. Ban, S. P. Alpay, and J. V. Mantese, *Integr. Ferroelectr.* **58**, 1281 (2003).
- ¹³S. Zhong, S. P. Alpay, and J. V. Mantese, *Appl. Phys. Lett.* **88**, 132904 (2006).
- ¹⁴T. B. Weston, A. H. Webster, and V. M. McNamara, *J. Am. Ceram. Soc.* **52**, 253 (1969).
- ¹⁵M. W. Cole, P. C. Joshi, and M. H. Ervin, *J. Appl. Phys.* **89**, 6336 (2001).
- ¹⁶M. W. Cole, E. Ngo, S. Hirsch, M. B. Okatan, and S. P. Alpay, *Appl. Phys. Lett.* **92**, 072906 (2008).
- ¹⁷S. Zhong, S. P. Alpay, M. W. Cole, E. Ngo, S. Hirsch, and J. D. Demaree, *Appl. Phys. Lett.* **90**, 092901 (2007).
- ¹⁸S. S. Gevorgian, T. Martinsson, P. L. J. Linner, and E. L. Kollberg, *IEEE Trans. Microwave Theory Tech.* **44**, 896 (1996).
- ¹⁹B. Su and T. W. Button, *J. Appl. Phys.* **95**, 1382 (2004).
- ²⁰D. M. Potrepka, S. Hirsch, M. W. Cole, W. D. Nothwang, S. Zhong, and S. P. Alpay, *J. Appl. Phys.* **99**, 014108 (2006).
- ²¹B. Acikel, Ph.D. thesis, University of California, Santa Barbara, 2002.